Determination of the quark-antiquark potential in the Hamiltonian formulation of the compact U(1) gauge theory.

Angelo Brade[1*]

[1*]Rheinische Friedrich–Wilhelms–Universität, Bonn.

Corresponding author(s). E-mail(s): s72abrad@uni-bonn.de;

Bachelorarbeit in Physik angefertigt im
Helmholtz-Institut für Strahlen- und Kernphysik

vorgelegt der Mathematisch-Naturwissenschaftlichen Fakultät
der
Rheinischen Friedrich-Wilhelms-Universität Bonn

Juli 2025

Contents

1 Introduction

The hamiltonian formulation of lattice gauge theory was first regarded as to costly for reasonable calculations. With the upcomming of quantum computers, we now expect a significant speedup of calculations that can be representet with states. The use of entanglement of these states promisses an exponential improvement. This fact moves the hamiltonian formulation in a point of interest again. For that reason we will revisit this formulation and implement the theory on a classical computer. I aim to give a good introduction such that other new students of the field will have a condensed understanding and intuition. The setup will be in the compact U(1) theory, truncated appropiately and reduced from the complete configuration space to a physical configuration space through Gauss's Law. For the numerical results we will take a look at the expectation value for the plaquette operator and finaly calculate the $q\bar{q}$ potential.

2 Theory

2.1 *Discretisation*

We start by discretising the positional space into sites and links. The sites are spaced by the lattice spacing a. To optain the continuum theory in the limit of $a \to 0$ we need to introduce the coupling constant g[1].

We associate each site with a corresponding positional vector $\vec{r} = (r_x, r_y)$. On the sites are the static charges $Q_{\vec{r}}$ positioned. We associate each link with a corresponding position $\vec{r}$ and a direction μ, where $-\mu$ is its opposite direction. For example with $\vec{r} = (1,2)$ and $\mu = x$ we would denote the link that points from the site $(1,2)$ to the x direction. We could denote the same link with $\vec{r} = (2,2)$ and $\mu = -x$.

On the links are the electric field operators $\hat{E}_{\vec{r},\mu}$ positioned. Each electric field $\hat{E}_{\vec{r},\mu}$ has the vector potential $\hat{A}_{\vec{r},\mu}$ as its canonical conjugate variable. Thus

$$[\hat{E}_{\vec{r}_i,\mu}, \hat{A}_{\vec{r}_j,\nu}] = i\delta^{(3)}(\vec{r}_i - \vec{r}_j)\delta_{\mu\nu}. \tag{1}$$

We construct a unitary operator $\hat{U}_{\vec{r}_j,\nu}$ (also called link operator) by using the vector potential as the generator in the Lie algebra $\mathfrak{g}$. Thus through the exponential mapping we get the elements of the Lie group G:

$$\hat{U}_{\vec{r},\mu} = e^{iag\hat{A}_{\vec{r},\mu}}. \tag{2}$$

The generated Lie group $G = \mathrm{U}(n)$ has the complex matrix elements $\hat{U}_{\vec{r},\nu}$ of dimension $n \times n$. By taking $n = 1$ we choose the U(1) theory. With restricting $\hat{A}_{\vec{r},\mu}$ to $ag\hat{A}_{\vec{r},\mu} \in [0, 2\pi)$ we arrive at the compact U(1) theory. Through eqs. (1) to (2) we get

$$[\hat{E}_{\vec{r}_i,\mu}, \hat{U}_{\vec{r}_j,\nu}] = \delta^{(3)}(\vec{r}_i - \vec{r}_j)\delta_{\mu\nu}\hat{U}_{\vec{r}_j,\nu}, \tag{3}$$

$$[\hat{E}_{\vec{r}_i,\mu}, \hat{U}^\dagger_{\vec{r}_j,\nu}] = -\delta^{(3)}(\vec{r}_i - \vec{r}_j)\delta_{\mu\nu}\hat{U}_{\vec{r}_j,\nu}\dagger. \tag{4}$$

To explore the effect of the operators on the states, we choose to be in the electric basis with the basis states $|e_{\vec{r}_i,\mu}\rangle$. The basis is made up of all possible states at the links. We optain

$$\hat{E}_{\vec{r}_i,\mu}\,|e_{\vec{r}_i,\mu}\rangle = e_{\vec{r}_i,\mu}\,|e_{\vec{r}_i,\mu}\rangle\,. \tag{5}$$

Furthermore with eqs. (3) to (5) we get

$$\hat{U}_{\vec{r}_i,\mu}\,|e_{\vec{r}_i,\mu}\rangle = |e_{\vec{r}_i,\mu} + 1\rangle \text{ and} \tag{6}$$

$$\hat{U}^\dagger_{\vec{r}_i,\mu}\,|e_{\vec{r}_i,\mu}\rangle = |e_{\vec{r}_i,\mu} - 1\rangle\,. \tag{7}$$

We see the unitary operators, also called link operators, act as ladder operators.

2.2 *Truncation*

Since each field can be any real value, there are infinitly many possible fields for each link, thus constructing an infinitly dimensional basis. To be computable we truncate the possbile values, such that the basis is finite.

Revisiting the elements of U(1) we see, that they live on the unit circle in the complex plane. By limiting the phase of our exponential mapping in equation eq. (2) to $[-l, l]$, the phase is now an element of $\mathbb{Z}_{2l+1}$. This also truncates the electric

field, such that $e_{\vec{r},\mu} \in [-l, l]$. The unitary operators, which as we saw act as ladder operators to the eigenstates, can now also be expressed as

$$\hat{U}_{\vec{r},\mu} \mapsto \begin{bmatrix} 0 & \dots & \dots & 0 \\ 1 & \dots & \dots & 0 \\ 0 & \ddots & \vdots & 0 \\ 0 & \dots & 1 & 0 \end{bmatrix}, \hat{U}^\dagger_{\vec{r},\mu} \mapsto \begin{bmatrix} 0 & 1 & \dots & 0 \\ 0 & \vdots & \ddots & 0 \\ 0 & \dots & \dots & 1 \\ 0 & \dots & \dots & 0 \end{bmatrix}.$$

The unitarity $\hat{U}_{\vec{r},\mu}\hat{U}^\dagger_{\vec{r},\mu} \neq \mathbb{1}$ for this is lost, but can be recovered in the continuum limit of $l \to \infty$. It is importend to point out, that we annihilate the first (last) state when using $\hat{U}^\dagger_{\vec{r}}$ ($\hat{U}_{\vec{r}}$).

2.3 *Hamiltonian*

The Hamiltonian for the system was orgininally formulated by Kogut and Susskind [2] and thus since known as the so called Kogut Susskind Hamiltonian. It reads

$$\begin{aligned} \hat{H} =& \hat{H}_E + \hat{H}_B + \hat{H}_m + \hat{H}_{\text{kin}} \text{ with} \\ \hat{H}_E =& \frac{g^2}{2} \sum_{\vec{r}} \left(\hat{E}^2_{\vec{r},x} + \hat{E}^2_{\vec{r},y} \right), \\ \hat{H}_B =& -\frac{1}{a^2 g^2} \sum_{\vec{r}} \text{Re}(\text{Tr}(\hat{P}_{\vec{r}})), \\ \hat{H}_m =& m \sum_{\vec{r}} (-1)^{r_x + r_y} \hat{\phi}^\dagger_{\vec{r}} \hat{\phi}_{\vec{r}} \text{ and} \\ \hat{H}_{\text{kin}} =& \frac{i}{2a} \sum_{\vec{r}} \left(\phi^\dagger_{\vec{r}} \hat{U}_{\vec{r},x} \phi_{\vec{r}+x} - \text{h.c.} \right) \\ & - \frac{(-1)^{r_x + r_y}}{2a} \sum_{\vec{r}} \left(\phi^\dagger_{\vec{r}} \hat{U}_{\vec{r},y} \phi_{\vec{r}+y} + \text{h.c.} \right). \end{aligned}$$

Firstly, lets get rid of the part we do not need. At the beginnen we introduced the static charges $Q_{\vec{r}}$. They are called static, since they can not move. We say that they have infinit mass, which implies they will not introduce any field and can not be moved. Thus the fermionic fields $\hat{\phi}_{\vec{r}}$ vanish at all $\vec{r}$. This premiss yields

$$\hat{H}_m = \hat{H}_{\text{kin}} = 0.$$

The computation can also be done with dynamic charges $\hat{q}_{\vec{r}}$ where the mass and kinetik Hamiltonian will make contributions. In this case a phenomena called doubling problem will rise. A common approach for this problem are staggered fermions. We will not take a look at this and stay in the pure gauge case, where only gauge fields exist.

Now we take a look at the two remaining terms. The electric Hamiltonian $\hat{H}_E$ and the magnetic Hamiltonian $\hat{H}_B$. For the latter one, we will take a look at the plaquette operator $\hat{P}_{\vec{r}}$. It is the smallest Wilson loop (a closed loop through the lattice on the link operators) and the oriented product of the link operators, i.e.

$$\hat{P}_{\vec{r}} = \hat{U}_{\vec{r},x} \hat{U}_{\vec{r}+x,y} \hat{U}^\dagger_{\vec{r}+y,x} \hat{U}^\dagger_{\vec{r},y}, \tag{8}$$

where e.g. $\vec{r} + x = (r_x + 1, r_y)$. We take the hermitian conjugate of the two latter link operators since all link operators only show in positiv x or y direction and when going through the plaquette we are going against the orientation of the two last link operators. Since the link operators are 1×1 matrices, the trace is just its argument. Taking the real part of an operator is not intuitive, so we rewrite it as

$$\text{Re}(\hat{P}_{\vec{r}}) = \frac{\hat{P}_{\vec{r}} + \hat{P}^\dagger_{\vec{r}}}{2}. \tag{9}$$

We see that by taking the hermitian conjugate of the plaquette operator, we just go through the plaquette the other way around.

The heuristic explaination of the form of the magnetic Hamiltonian is the following: The plaquettes, as they are closed loops, are essentially conductor loops that introduce a magnetic moment by Farady's law, that is then measured by the magnetic hamiltonian.

Now we take a look at the electric Hamiltonian. It is essentially the sum over each lattice site over the square of the electric field. Here we use the electric field operators $\hat{E}^2_{\vec{r},\mu}$ and have to do no modifications, since we work in the electric basis.

So at the end, the total hamiltonian reads

$$\hat{H} = \frac{g^2}{2} \sum_{\vec{r}} \left(\hat{E}^2_{\vec{r},x} + \hat{E}^2_{\vec{r},y} \right) - \frac{1}{2a^2 g^2} \sum_{\vec{r}} \left(\hat{P}_{\vec{r}} + \hat{P}_{\vec{r}} \right).$$

2.4 *Gauss's Law*

A constraint, that limits our possible states is Gauss's Law. It constraints by the number of lattice sites, such that some links are dependent on other links. The links, that are dependent on

other links, are called fixed links. The links that are independent, are called dynamic links. The formulation reads

$$\left[\sum_{\mu=x,y}\left(\hat{E}_{\vec{r},\mu}-\hat{E}_{\vec{r}-\mu,\mu}\right)-\hat{q}_{\vec{r}}-Q_{\vec{r}}\right]|\Psi\rangle=0. \quad (10)$$

Here we sum over all electric field operators that are linked to a site $\vec{r}$ and are expecting them to be the same as the charge deposited on the site. Only those lattice states $|\Psi\rangle$, which produce this relation, are thus physicaly possible. They live in the physical space $\mathcal{H}_{\text{ph}}$:

$$|\Psi\rangle \in \mathcal{H}_{\text{ph}}, \quad (11)$$

where we denote by $\mathcal{H}$ the space in which a lattice configuration lives. Here the physical configuratino Hamiltonian $\mathcal{H}_{\text{ph}}$ is a subspace of the the complete configuration Hamiltonian $\mathcal{H}$.

We will use this dependence of the fixed links, to represent them in terms of the dynamic links. This can by done analyticaly on paper or with the library `sympy`[3] in python. For convenience, we will use the latter. It will be used to solve the generated linear system of eqations.

3 Implementation

The code for this work can be accessed over this git hub link: https://github.com/valentino-dev/Bachelorthesis/tree/main/src.

3.1 *Matrix representation*

For the implementation we construct the lattice and place all operators on thier links. Then we calculate each entry while we can directly use the fact, that we are in the electric basis:

$$\begin{aligned}\langle i|\hat{H}|j\rangle =& \frac{g^2}{2}\sum_{\vec{r}}\left(e^2_{\vec{r},x}+e^2_{\vec{r},y}\right)\delta_{ij}\\ &-\frac{1}{2a^2g^2}\sum_{\vec{r}}\langle i|\left(\hat{P}_{\vec{r}}+\hat{P}_{\vec{r}}\right)|j\rangle\end{aligned}$$

with $|i\rangle \in \mathcal{H}$. Let us calculate $\langle i|\hat{P}_{\vec{r}}|j\rangle$:

$$\begin{aligned}\langle i|\hat{P}_{\vec{r}}|j\rangle &= \langle i|\hat{U}_{\vec{r},x}\hat{U}_{\vec{r}+x,y}\hat{U}^\dagger_{\vec{r}+y,x}\hat{U}^\dagger_{\vec{r},y}|j\rangle\\ &= \langle i|\,|e^{(j)}_{\vec{r},x}+1\rangle\otimes|e^{(j)}_{\vec{r}+x,y}+1\rangle\\ &\quad\otimes|e^{(j)}_{\vec{r}+y,x}-1\rangle\otimes|e^{(j)}_{\vec{r},y}-1\rangle\\ &\quad\bigotimes_{\text{rest links}}|e^{(j)}_{\vec{r}',\mu'}\rangle\\ &= \langle i\,|\,k\rangle\\ &= \delta_{ik}\end{aligned}$$

The formulation reads as following: State $|j\rangle$ will be transformed by the plaquette operator $\hat{P}_{\vec{r}}$ into some state $|k\rangle$. Thus $\hat{P}_{\vec{r}}$ gets an entry at row $\langle i|$ and collumn $|j\rangle$ if, and only if, state $|j\rangle$ is transformed into state $|i\rangle$. Now knowing $\hat{P}_{\vec{r}}$ in matrix representation, trivialy yealds $\hat{P}^\dagger_{\vec{r}} = \left(\hat{P}^*_{\vec{r}}\right)^T$ and with it the matrix representation of the magnetic hamiltonian.

On a side note, going through states $|i\rangle$ means, counting up in base $2l+1$ with the link states $|e_{\vec{r},\mu}\rangle$ being the "digits". This is schematicly illustrated in table 1.

i	$\lvert i\rangle$
0	$(-l,-l,\ldots,-l,-l)$
1	$(-l,-l,\ldots,-l,-l+1)$
$\vdots$	$\vdots$
$2l+1$	$(-l,-l,\ldots,-l,l)$
$2l+2$	$(-l,-l,\ldots,-l+1,l)$

Table 1: Scheme of state indexing.

With this proccedure we would have to check every combination of states $\langle i|$ and $|j\rangle$, which would be very costly. Instead we just calculate the transformation $\hat{P}_{\vec{r}}|j\rangle = |k\rangle$ for every state $|j\rangle$ and set $(\hat{P}_{\vec{r}})_{kj} = 1$, i.e. having a contribution at row $\langle k|$ and collumn $|j\rangle$.

Gauss's Law not only restricts the electric operators, but also the corresponding link operator on the same link. But here Gauss's Law does not impose a dependency, but rather the dynamical link operators automticly produce physical states, where as the fixed link operators do not act anymore on our physical space, which is why we can ignore the fixed ones. Thus with plaquette operators we would normaly have allways four link operators, we now get plaquette operators that are a product of any number of link operators ranging from 0 to 4. Which number it will be is then dependent on the position of the plaquette. When a plaquette does not go throught any dynamical link

operators, it will never produce a physical state and thus can be entirely ignored.

3.2 *Exact diagonalisation*

Now having the total hamiltonian in matrix representation, we can use diagonalisation to compute the eigenvalues and eigenstates. For that the library `scipy`[4] was used. It provides the method `scipy.sparse.linalg.eigsh`, which is an eigensolver, which can be used to calculate the k smallest algebraic (SA) eigenvalues. It can use hermitian sparse row matrices which speed up the process drasticly in comperison to dense non hermitian matrices.

3.3 *Computational ressources*

The disadvantage of the hamiltonian formulation of the lattice gauge theory, is it need for computational ressources, since every link can be in $2l+1$ states and in two dimensions, we have two links for every site. Now depending if we have periodic boundary conditions (PBC) or not, we have the links that connect the sites of opposides sides or not. The exact number of states for a square $n \times n$ lattice with PBC would be $N = (2l+1)^{2n^2}$ and without PBC $N = (2l+1)^{2(n^2-n)}$. But since we are only interested in physical states, each site imposes a Gauss's Law and thus restricts the number of total states to only the physical states. So each site introduces a constraint

$$\sum_{\mu=x,y} \left(E_{\vec{r},\mu} - E_{\vec{r},-\mu}\right) = Q_{\vec{r}}. \tag{12}$$

To check if they are linearly independend we sum over all sites and get

$$\sum_{\vec{r}} \sum_{\mu=x,y} \left(E_{\vec{r},\mu} - E_{\vec{r},-\mu}\right) = \sum_{\vec{r}} Q_{\vec{r}}. \tag{13}$$

We see, that only if the total sum of charges is non zero, we have linear independency. But if the total sum is zero, we have a redundent constraint, which reduces the total number of constraints from n^2 to n^2-1. From now on we assume that the total charge is allways zero, since we only work with no charges or with a pair of opposite charges.

This limits our total number of electric operators $N_E = 2n^2$ to only a fraction that is dynamic: $N_{E,\text{dyn}} = n^2+1$. For a lattice without PBC we get $N_E = 2(n^2-n)$ and $N_{E,\text{dyn}} = n^2-2n+1$. The number of physical states for a lattic with PBC is thus

$$N_{\text{ph}} = (2l+1)^{n^2+1}. \tag{14}$$

And without PBC

$$N_{\text{ph}} = (2l+1)^{n^2-2n+1}. \tag{15}$$

Since from our calculations we will receive matrices with size $N_{\text{ph}} \times N_{\text{ph}}$, the number of physical states will be a good measure for computation time. To get an idea on some realistic lattices and thier number of physical states, see table 2.

lattice	N_{ph}
2x2, no PBC and $l=1$	3
2x2, PBC and $l=1$	243
2x2, PBC and $l=7$	759×10^3
3x3, PBC and $l=1$	19.7×10^3
3x3, PBC and $l=2$	1.95×10^6
3x3, PBC and $l=4$	387×10^6

Table 2: Lattice sizes and thier number of physical states.

We can use to our advantage, that most of the elements of the hamiltonian are zero and only a few are non-zero entries. Thus instead of storing all elements, even those that are zero, we only store the non-zero entries by storing its row and collumn position and the value. This is called a Compressed Sparse Row (CSR) matrix and will reduce the needed memory drasticly.[1]

Now that we have a little intuition for the complexity, we continue with the actual computation times. We do the calculations on the supercomputer Marvin of the University of Bonn. Building the Hamiltonian for the 3×3 lattice with PBC and $l=1$ took 1.5 s and diagonalizing it to $g=1$ took 0.27 s.[2] B

To utilize the HPC to capacity, multiprocessing was introduced. The code was rewriten, such that the calculation of the elements is spreaded onto the threads, without spreading to thinly, i.e. launching new threads takes more time then

[1] Nevertheless a Hamiltonian of a 3×3 lattice with PBC and $l=3$ takes about 150 GB to be stored.

[2] This assessment was done by using one node with two CPUs of the type Intel Xeon 'Sapphire Rapids' 48-core/96-thread 2.10GHz.

truncation l	building $\hat{H}$	diagonalizing
1	1.5 s	0.27 s
2	110 s	11 minutes
3	1 h	5 h

Table 3: Computation time for a 3×3 lattice with PBC.

processing, or to dense, i.e. not all cores are utilized.

4 Results

4.1 *Plaquette expectation value*

As first comparison and comfirmation of our setupt, we will calculate the plaquette expectation value. It is definied as the following:

$$\langle P \rangle = \left\langle \sum_{\vec{r}} \frac{P_{\vec{r}} + P_{\vec{r}}^{\dagger}}{2} \right\rangle. \tag{16}$$

From the scaling of the Hamiltonian in respect to g we would expect $\lim_{g\to\infty} \langle P \rangle = 0$ and $\lim_{g\to 0} \langle P \rangle = 1$. fig. 1 is the result of the calculation and as we see, it behaves as expected. An interesing but not

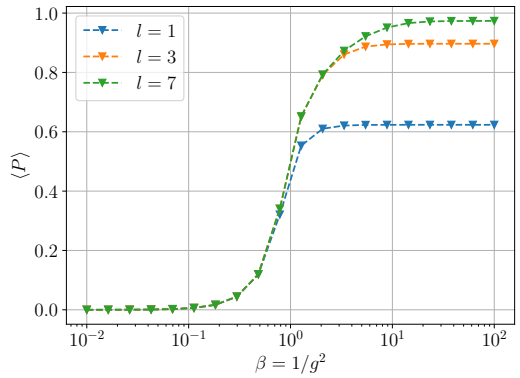

Figure 1: plaquette expectation values for a 2×2 lattice with PBC.

suprising observation is the convergance of the expectation value to 1 for large β with the order of truncation. Thus using large l is favourable.

As a next step we look at the next larger lattice and use dimensions of 3×3. fig. 2 shows the results. Here we want to focus only on larger β.

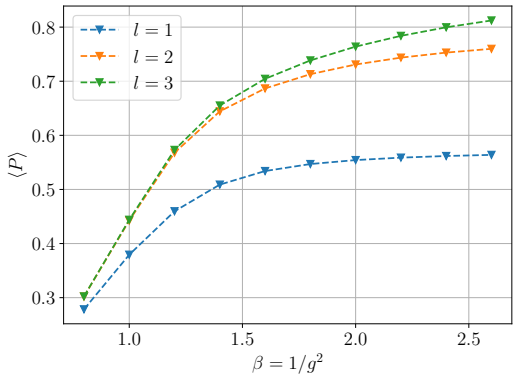

Figure 2: Plaquette expectation values for a 3×3 lattice with PBC.

Here we can also confirm the convergence to 1 as we increase β and the truncation. Especially this Figure and its results are direcetly comparable to the figure from Arianna Crippa et al. (2024)[5]

4.2 *Quark-Antiquark potential*

Now for calculating the quark antiquark potential we need to subtract the energy of the chargeless lattice H_0:

$$V = \langle H \rangle - \langle H_0 \rangle \tag{17}$$

with H beeing the lattice with the desired charge. For our porpose we place one charge in the buttom left corner and place the opposite charge at a lattice site with desired distance. We also want to study the effect of diffrent setups on charge pairs with the same distance. Thus we will vary the truncation l from 1 to 3 and also compare the orginal 3×3 lattice with no PBC with a lattice with PBC and a lattice with dimensions 4×4. With these diffrent setups we optain fig. 3. Throughout this section this is the central Figure, that we will discuss. Firstly we take a look at most basic setup: A 3×3 lattice with no PBC and a trancation of $l = 1$. Here we can see the basic behaviour for increasing distance r. The potential raises, which hints that we experience confienemnt.

Now we watch what happens if we vary diffrent lattice parameters. If we choose a diffrent truncation l, here 2 and 3, the potential has the same behaviour but is negativly shifted. This is to be expected, since as we approach continuum, and the lattice fragments vanish, we also approach the true

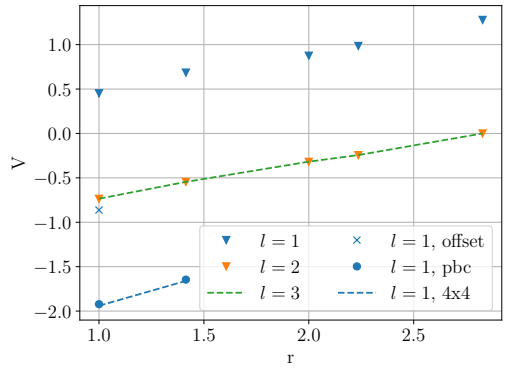

Figure 3: Quark-Antiquark potential for diffrent but comparable setups at $g = 1$. By default 3×3 dimensions and no PBC, if not stated otherwise.

lowest energie eigenstate. We also see, that the diffrence from $l = 1$ to $l = 2$ is quite signifacant, but the next stept, from $l = 2$ to $l = 3$, is barely notacable. This shows, that that a truncation of at least $l = 2$ is favourable.

For the next comparison we watch what happens if we do not set the charge pair at the rim, but at the center. We would also expect a negative shift of the potential, since at the rim we would never see the translational invariance of the continuum. Only at the center we could get an approximate translational invariance. The scene is sketched in fig. 4. The normal setup is used for our initial calculation with $l = 1$ at $r = 1$ (upside down triangle). The potential of the offset setup is now depicted by the blue cross in fig. 3. We can see that indeed the potential also gets a negative shift. An interesting side note is that it shifts even further then the improvement in truncation.

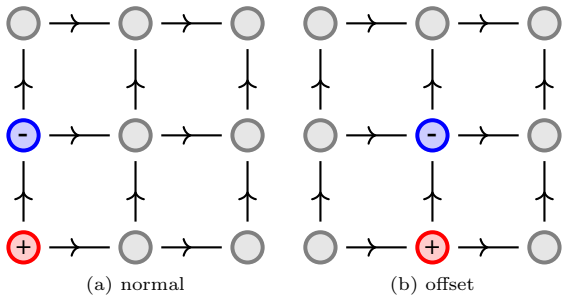

Figure 4: 3×3 lattice with two charge pairs of same distance but diffrent position.

A clever way to avoid rims, is to use periodic boundary conditions (PBC). The disadvantage is that the shortest path is not allways the path through the center links, but through the links that are introduced by the PBC. This limits our possible charge pair setups, since allready for a 3×3 lattice with PBC, there are only two diffrent setups. All other setups can be created by translation and rotation of those two. They are depicted in fig. 5 We again expect a negative shift, since we have translational invariance. Thou we have translational invariance, it is not the same as in the continuum limit, since with PBC the paths also loop around through the links that are introduced by the PBC. Those paths are also colored in fig. 5. The resulting potentials are marked with circles in fig. 3. We see the expectations are fullfilled. But the shift is even more significant then just centering the pair. Cause of this is probably the fact that with our offset setup, with a 3×3 lattice and no PBC, the one charge was still placed at a rim site. Unfortunately this is not to be avoided with a 3×3 lattice.

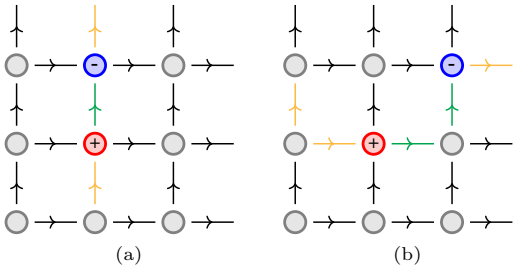

Figure 5: Two 3×3 lattices with PBC and a charge pair with shortest distance (a) and second shortest distance (b). Colored paths: shortest (Green) and second shortest (Yellow) path.

For the continuation of our previous comparison we now use a 4×4 setup. We again place the charge pairs centered, as shown in fig. 6. Again only two setups are possbile, where no charge is on the rim. All other can be optained by rotating the lattice. We expect a negative shift, since we approach translational invariance.

The potential is marked with a dashed line in fig. 3. As we see, compared to the inital setup we get an improvement. But the diffrence to the 3×3 lattice with PBC is very small. It does not

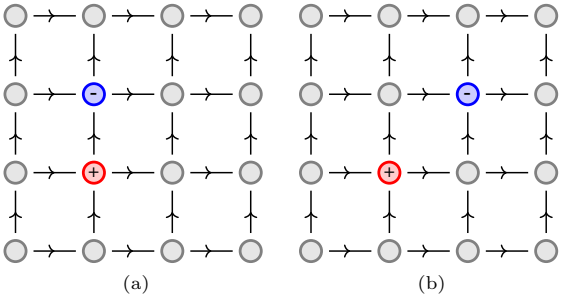

Figure 6: Two 4×4 lattices with two charge pairs with shortest distance (a) and second shortest distance (b).

matter too much, that a lattice has PBC. The only importance lies in the fact, that no charges are on the rim. It would be interesting to see, if this behaviour still holds for larger lattice sizes. Unfortunately, computing those is currently not feasible.

At last we will take a look at diffrent coupling regemes. We will see that allready little diviations from the original coupling of $g = 1$ show new behaviours. Therefore we choose $g = 0.8$ and $g = 1.2$ and compare thier potentials to the orginal. First we compute $g = 1.2$ and get fig. 7. We see, that

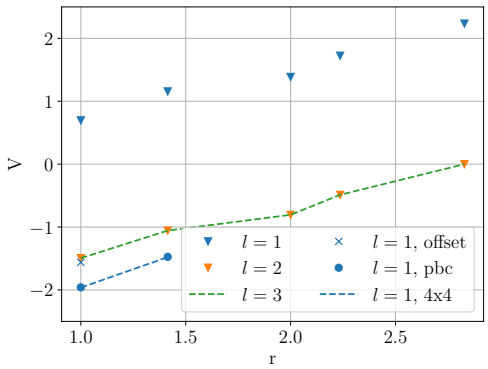

Figure 7: Quark-Antiquark potential for diffrent but comparable setups at $g = 1.2$. By default 3×3 dimensions and no PBC, if not stated otherwise.

the potential is not so linear any more and begins to form steps, which shows that for large coupling the lattice fragments are intensified. We also see a larger seperation of the truncation $l = 2$ and $l = 3$ in respect to $l = 1$. Furthermore the potential of the 4 × 4 lattice or the 3 × 3 lattice with PBC is unchanged. It seems as if the truncation gains importains for larger couplings, where as the lattice size keeps its importance as is. Interestingly the potential for the centered charge pair ($l = 1$, offset) moves with the $l = 2$ and $l = 3$ truncated potentials.

Second we compute $g = 0.8$ and get fig. 8. Here

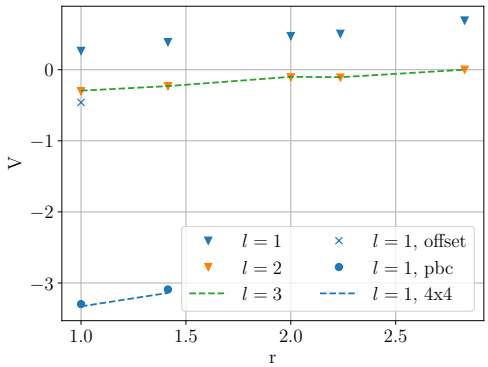

Figure 8: Quark-Antiquark potential for diffrent but comparable setups at $g = 0.8$. By default 3×3 dimensions and no PBC, if not stated otherwise.

the $l = 2$ and $l = 3$ truncated potentials decrease in seperation in respect to the $l = 1$ truncated potential. The potential for the 4 × 4 and the 3 × 3 lattice with PBC start to increase in seperatin in respect to the 3 × 3 lattice with PBC and truncation $l = 1$. This indicates, that as the coupling decreases the truncation looses in importance and the lattice volume, i.e. the number of total links, increases. The potential with the centered charge pair moves just as with large couplings with the truncation of $l = 2$ and $l = 3$. This shows, that not the fact, that no charge is placed on the rim is important, but the actual lattice volume.

5 Conclusion

With the advancemend of quantum computers, the Hamiltonian formulation of gauge theorys gains interest again. For this we started by constructing a lattice in the compact U(1) formulation where we placed electric and link operators on the links and static charges on the sites. The Kogut Susskind Hamiltonian was modefied to be

in pure gauge, such that there are no fermionic fields. A truncation l was introduced to render the configuration Hamiltonian finite. Further more we used Guass Law to limit our total number of configuration states to a physical subspace that later on reduces needed computational ressources.

With this theoretical setup the numerical implementation started by calculating the matrix elements for the electic and magnetic hamiltonian. Here we used the electic basis and the fact that the link operator is the canonical conjugat to the electic operator, to optain the action of our operators on our states. We briefly dived into computational ressources and build an intuition for the needed computation times.

We computed the plaquette expectation value for comparision with previous work and to confirm the correctness of the setup. Finally we computed the quark-antiquark potential by placeing two static charges. Here we measured the potential in relation to distance and experienced confinement. Further more we disscussed the influence of diffrent lattices on the potential by varying the truncation, lattice size and introducing PBC.

6 Acknowledments

I want to thank Emil Rosanowski from the Funcke research group, Allesio Negro and Paul Ludwig from the Urbach research group, and ofcause Carsten Urbach himself, from the University of Bonn, for allways beeing open for disscussion and inspiration. I also want to thank Arianna Crippa for her code from [5] to estableash first intuition. The author gratefully acknowledges the access to the Marvin cluster of the University of Bonn.

References

[1] Kogut, J.B.: An introduction to lattice gauge theory and spin systems. Rev. Mod. Phys. **51**, 659–713 (1979) https://doi.org/10.1103/RevModPhys.51.659

[2] Kogut, J., Susskind, L.: Hamiltonian formulation of wilson's lattice gauge theories. Phys. Rev. D **11**, 395–408 (1975) https://doi.org/10.1103/PhysRevD.11.395

[3] Meurer, A., Smith, C.P., Paprocki, M., Certík, O., Kirpichev, S.B., Rocklin, M., Kumar, A., Ivanov, S., Moore, J.K., Singh, S., Rathnayake, T., Vig, S., Granger, B.E., Muller, R.P., Bonazzi, F., Gupta, H., Vats, S., Johansson, F., Pedregosa, F., Curry, M.J., Terrel, A.R., Roučka, v.p., Saboo, A., Fernando, I., Kulal, S., Cimrman, R., Scopatz, A.: Sympy: symbolic computing in python. PeerJ Computer Science **3**, 103 (2017) https://doi.org/10.7717/peerj-cs.103

[4] Virtanen, P., Gommers, R., Oliphant, T.E., Haberland, M., Reddy, T., Cournapeau, D., Burovski, E., Peterson, P., Weckesser, W., Bright, J., van der Walt, S.J., Brett, M., Wilson, J., Millman, K.J., Mayorov, N., Nelson, A.R.J., Jones, E., Kern, R., Larson, E., Carey, C.J., Polat, İ., Feng, Y., Moore, E.W., VanderPlas, J., Laxalde, D., Perktold, J., Cimrman, R., Henriksen, I., Quintero, E.A., Harris, C.R., Archibald, A.M., Ribeiro, A.H., Pedregosa, F., van Mulbregt, P., SciPy 1.0 Contributors: SciPy 1.0: Fundamental Algorithms for Scientific Computing in Python. Nature Methods **17**, 261–272 (2020) https://doi.org/10.1038/s41592-019-0686-2

[5] Crippa, A., Romiti, S., Funcke, L., Jansen, K., Kühn, S., Stornati, P., Urbach, C.: Towards determining the (2+1)-dimensional Quantum Electrodynamics running coupling with Monte Carlo and quantum computing methods (2024). https://arxiv.org/abs/2404.17545

Ich versichere, dass ich diese Arbeit selbstständig verfasst und keine anderen als die angegebenen Quellen und Hilfsmittel benutzt sowie die Zitate kenntlich gemacht habe.

Bonn, ...
Datum

.....,
Unterschrift

1. Gutachter: Prof. Dr. Carsten Urbach
2. Gutachterin: Jun.-Prof. Dr. Lena Funcke